SPE

Society of Petroleum Engineers

SPE 18741

Sixth SPE Comparative Solution Project: A Comparison of Dual-Porosity Simulators

by A. Firoozabadi, Norsk Hydro A/S, and L.K. Thomas, Phillips Petroleum Co.

SPE Members

This paper was prepared for presentation at the SPE Symposium on Reservoir Simulation in Houston, TX, February 6–8, 1989.

ABSTRACT

Two problems for the comparison of fractured reservoir models are presented. The first problem is a simple single block example. The second problem is a more complicated cross-sectional example. The cross-sectional example has been developed to simulate depletion, gas injection and water injection cases.

In selecting the problems for the present Comparative Solution Project, various aspects of the physics of multiphase flow in fractured porous media have been considered. The question of fracture capillary pressure and its influence on reservoir performance has been addressed by including cases with zero and non-zero gas-oil capillary pressure in the fractures.

Ten organizations participated in the Sixth Comparative Solution Project. Most of the current techniques in dual-porosity simulation are represented in the results of the participants.

INTRODUCTION

In recent years, there has been an increased interest in the simulation of naturally fractured petroleum reservoirs. For the present SPE Comparative Solution Project, reservoir test problems have been designed to illustrate various aspects of the physics of multiphase flow in fractured reservoirs as well as the modelling techniques to account for capillary and gravity forces. The approach to the solution of the problems has been limited to dual-porosity models.

An important element in simulating a fractured reservoir using a dual-porosity technique is the proper calculation of the fluids exchange between the matrix blocks and the fractures. In the conventional approach, the transfer term for a particular phase is directly related to the shape factor, σ, fluid mobility and potential difference between the matrix and fracture[1]. Shape factors have been developed based on first-order finite-difference approximations[2] and by matching fine grid multiphase simulations of matrix-fracture flow[3].

In most dual-porosity models, the matrix block heights are assumed to be at the same depth as the corresponding fracture blocks, and therefore, gravity has no explicit effect on the fluid exchange between the matrix and the fracture. Pseudo capillary pressures have been used to account for the effect of gravity[3]. The gravity segregation concept has also been used to compute the fluid levels in the matrix and fractures to account for the gravity contribution[4,5].

References and illustrations at end of paper.

Another consideration in dual-porosity models is the accounting of saturation distribution in a matrix block. Since the saturation is evaluated at the center of a gridcell, it represents an average value for that cell. The pseudo capillary pressure concept has been used to account for both gravity effects and non-uniform saturations within a matrix block[3,6,7]. The method of subdomain discretization has also been applied to this problem[8,9]. In this approach the matrix is divided into a number of gridcells and pressures and saturations are calculated for each gridcell. The subdomain approach can also take care of transient effects. These effects may not, however, be important in field scale problems.

Fracture capillary pressure is assumed to be zero in most dual-porosity models. A recent paper questions the validity of zero fracture capillary pressure[10]. In selecting the problems for the present Comparative Solution Project, the influence of fracture capillary pressure on reservoir performance has been addressed by including cases with zero and non-zero gas-oil capillary pressure in the fractures. The non-zero fracture capillary pressures are not based on any actual measurements, but are intended as a parameter for sensitivity studies. The variation of gas-oil interfacial tension with pressure has also been incorporated in the problems. Gas-oil capillary pressure is directly related to interfacial tension, and therefore, the gas-oil capillary pressure should be adjusted according to the ratio of interfacial tension at pressure divided by interfacial tension at the pressure at which capillary pressures are specified.

PROBLEM STATEMENT

We have selected two problems for the comparison of fractured reservoir models: A single block example, and a more complicated cross-sectional example. The cross-sectional example has been developed to simulate depletion, gas injection and water injection cases.

Basic PVT data for the above cases was taken from Ref. 3. The rock-fluid data with the exception of the matrix water-oil capillary pressure was also taken from the same reference. Table 1 gives the matrix water-oil capillary pressure data. Matrix block shape factors have been specified for use in simulators which directly input this variable (see Table 2).

Single Block Studies

The single block simulation is a study of gas-oil gravity drainage at

4500 psig [31.0 MPa] for a cubic matrix block with dimensions of 10 x 10 x 10 ft. [3.05 x 3.05 x 3.05 m]. A one cell dual-porosity run was made for this case. Two runs were reported. The first run with a zero fracture capillary pressure, and the second run with a constant fracture capillary pressure of 0.1 psi [0.69 kPa]. These runs were terminated at 5 years.

Cross-Sectional Studies

The layer description for the cross-sectional studies is given in Table 3. In all studies, the injection well was located at I=1, and the production well was located at I=10. Input data for each study is given below.

Depletion. Depletion runs were carried out to a maximum of ten years or whenever production declined to less than 1 STB/D [0.16 m^3/D]. The production well has a maximum rate of 500 STB/D [80 m^3/D], and it was limited by a maximum drawdown of 100 psi [689 kPa]. This well was perforated only in the bottom layer.

Two runs were made: the first with zero fracture capillary pressure, and the second using fracture capillary pressure data from Table 4. These data are reported at the bubble point pressure of 5,545 psig [38.23 MPa] and were adjusted for the effect of pressure on interfacial tension.

Gas Injection - For these runs 90 percent of the gas produced from the previous time step was reinjected. The injection well was perforated in layers 1, 2, and 3. The production well was perforated only in layers 4 and 5, and was constrained by a maximum drawdown of 100 psi [689 kPa]. A maximum rate of 1000 STB/D [160 m^3/D] was set. The minimum cut off rate was 100 STB/D [16 m^3/D].

Two runs were made: the first with zero fracture capillary pressure, and the second with fracture capillary pressure data from Table 4 adjusted for the pressure effect.

Water Injection - In this run, water was injected at time zero at a maximum rate of 1750 STB/D [280 m^3/D] and was constrained by a maximum injection pressure of 6100 psig [42.06 MPa]. The production rate was set equal to 1000 STB/D [160 m^3/D] of total liquid(s) (water and oil). The injection well was perforated in layers 1, 2, 3, 4 and 5, and the production well was perforated in layers 1, 2 and 3. A total run time of 20 years was reported.

For the above two problems, the following data were specified to control time step sizes.

Maximum saturation change	= 0.1
Maximum pressure change	= 500 psi [3.45 MPa]
Maximum saturation pressure change	= 500 psi [3.45 MPa]

Maximum time step increment for the gas injection and water injection cases was set to 0.25 years. Maximum time step increment for the depletion cases was set to 0.1 years to minimize time truncation error.

REPORTING RESULTS

For the single block gas-oil gravity drainage runs, oil recovery vs. time at 0.25 year increments was reported.

The following results were reported for the cross-sectional runs.

- Oil production rate, gas-oil ratio (GOR) and pressure at gridblock (5, 1, 1) each year for the depletion and gas-injection runs.
- Fracture and matrix gas saturations at 2, 5, 10 and 20 years for the column of blocks at I=5, and K=1 to 5 for the gas injection case with the non-zero fracture capillary pressure.
- Oil production rate, and water cut each year for the water injection run.
- Total number of time steps and global iterations for all runs.

DESCRIPTION OF MODELS USED

Ten organizations participated in the Sixth SPE Comparative Solution Project (see the Appendix). A short description of the models used by these organizations is given below.

Chevron Oil Field Research Company (Chevron)

Chevron's naturally fractured reservoir simulator, NFRS, was used to solve the problems of the Comparative Solution Project. This simulator is based on the methodology outlined in Ref. 11. NFRS avoids the use of shape factors by using cylindrical matrix blocks that may be discretized in the r and z directions[8]. Fluid exchange between fracture and matrix is allowed through top, bottom, and side faces of the matrix blocks.

Two cells were used to solve the single matrix problem: one cell containing a gas injector at 0.5 PV/day, and the second cell containing a producer at 4500 psig [31.0 MPa].

A sensitivity analysis showed that vertical discretization of matrix blocks had a strong effect on oil recovery. This effect was strongest in the gas injection example with zero fracture capillary pressure. As a result of the sensitivity analysis the single block problem, depletion, and gas injection cases were run using 4 matrix block layers and the water injection case was run with undiscretized matrix blocks.

Computer Modelling Group (CMG)

CMG used the IMEX model which is both a single-porosity and a dual-porosity/dual-permeability, four-component, adaptive-implicit reservoir simulator. For the dual-porosity option, IMEX allows the discretization of the matrix blocks into subblocks either in the nested format[9] for the representation of transient effects or in the layer format for the representation of gravity effect[12].

For the problems of this Project, the dual-porosity option with the subdomain approach was used to represent the matrix-fracture fluid transfer calculations. In this model, the matrix block dimensions are entered directly, and no shape factor is required. Since the matrix block is discretized, the fluid transfer between the matrix and the fracture is believed to be properly represented by difference equations. Within a given gridblock, gravity segregation is assumed in the fractures. All runs were performed with five subdomain blocks per gridcell. A five-point differencing scheme with single-point upstream weighted mobility was used.

DANCOMP A/S

The DANCOMP/RISO simulator was used for the test examples of the present Project. This is a three-phase, 3D isothermal model which can run in either black-oil or compositional modes with a dual-porosity/dual-permeability option.

Space discretization is performed by the integral finite difference technique to avoid reference to a specific coordinate system. The time integration method is fully implicit, and the time step is adjusted automatically to maintain a specified accuracy. The resulting nonlinear system of equations are solved by the Newton-Raphson method. The system of linear equations are solved either by a direct band solver or by an iterative sparse matrix solver.

In the DANCOMP/RISO model, the saturation gradients within the matrix blocks for an imbibition process are taken into account. The imbibition is modelled as a diffusion process with capillary forces as the driving mechanism[13]. The corresponding diffusion equation is solved either numerically or analytically. Recovery from gas-oil gravity-drainage is found by considering, 1) matrix blocks above the gas-oil contact, 2) matrix blocks in the gas-oil contact zone, and 3) matrix blocks below the gas-oil contact. In water-oil cases a capillary continuity between adjacent horizontal matrix blocks in the same gridcell is assumed.

Exploration Consultants Limited (ECL)

ECL used the Eclipse model in dual-porosity mode. This model required two simulation cells to represent each gridblock volume; one each for the rock matrix and the fracture properties. In the dual-porosity mode, the shape factor in the transfer function term was computed from Eq. 5 of Ref. 1.

Eclipse is a fully implicit program and reinjects a fraction of the phase production or reservoir voidage from the current timestep to model pressure maintenance schemes. This approach has been used in the gas injection runs rather than reinjecting gas from the previous time step.

In all the runs, the Eclipse iterative solution techniques of nested factorization for the linear equations and Newtons method for the non-linear equations were used. In the present drawdown control in Eclipse the maximum drawdown was converted to a maximum liquid rate which may not be exceeded. The target liquid rate was updated at each non-linear iteration. Limiting the number of iterations for which the target is updated would reduce the number of iterations at the expense of accuracy. Eclipse does not have a pressure dependent gas-oil capillary pressure option at present. Therefore, gas-oil capillary pressures at 4000 psig [27.60 MPa] were used for the gas injection and depletion runs.

FRANLAB

FRAGOR was used by FRANLAB to simulate the test examples. This model is a three-phase, 3D black-oil, pseudo and fully compositional simulator with a dual-porosity/dual-permeability option. Ref. 14 outlines the main features of the model.

The matrix fracture flows are computed through the six faces of the central block of each cell. Gravity, capillary, and viscous forces are included in the dual-porosity options.

Numerical solution schemes such as fully implicit and adaptive implicit techniques are available in FRAGOR.

In using the FRAGOR model, no attempt was made to introduce any correction factor or pseudofunctions to correct for the effects of an undiscretized matrix block.

Japan Oil Engineering Company (JOE)

The model used by JOE has been developed jointly by Japan Oil Engineering Co., and Japan National Oil Corporation (JNOC). The runs were performed using fracture-matrix fluid transfer of Ref. 1. The model uses a finite-difference spatial discretization in which flow terms are weighted upstream, and applies a fully implicit backward Eular method for the time discretization. Non-linear iterations are performed using the Newton-Raphson technique. Various options for the matrix-fracture transfer function are currently being tested.

Marathon Oil Company

Marathon's fractured simulator is a fully implicit, three-phase, 3D model. Matrix-fracture fluid transfer function for each phase is based on the transmissibilities of Ref. 1 with upstream mobilities. In running the example problems of the current Project D_f was assumed to be equal to D_{ma}.

In this simulator, pseudo capillary pressure curves were used to simulate the gravity forces[7].

For the gas-oil system, a pseudo fracture capillary pressure was found for each block size that would allow a dual-porosity, single node model to match oil recovery from a vertical dual-permeability fine grid model. This match was obtained at a constant pressure of 4500 psig [31.03 MPa]. Matrix capillary pressure was unchanged. For all other pressures, the matrix capillary pressure (adjusted by the interfacial tension ratio) was integrated to determine an equilibrium gas saturation for each block height. Pseudo interfacial tension ratios for the fracture were calculated at each pressure for each block size, such that when multiplied by the maximum base fracture pseudo capillary pressure, the matrix and fracture capillary pressures would be equal at $S_{gf} = 1$ and $S_{gm} = S_{ge}$. S_{ge} is the equilibrium matrix gas saturation determined by integration of the capillary pressure curve at each pressure and for each matrix block height. The above procedure was used for both the zero and non-zero fracture capillary pressure cases.

For the water-oil case, pseudo fracture capillary pressures were developed for each matrix block size at 6000 psig [41.36 MPa] such that a dual-porosity model would give the recovery as determined from fine grid simulations.

For both water-oil, and gas-oil cases, matrix shape factor was computed from $\sigma = 12/L_{ma}^2$.

Phillips Petroleum Company

Phillips simulator is a fully implicit, 3D, three-phase single or dual-porosity model. For dual-porosity simulations primary flow in the reservoir occurs within the fractures with local exchange of fluids between the fracture system and matrix blocks. The matrix-fracture transfer term is based on an extension of the equation developed by Warren and Root[15] and accounts for capillary pressure, gravity and viscous forces. Matrix unknowns are implicitly evaluated as a function of fracture unknowns. The matrix-fracture flow equation accurately matches detailed simulations of multi-phase flow processes.

Provisions are included for modelling the gravity term; for properly calculating relative permeabilities as a function of both up and down stream conditions and hysteresis; and for evaluating the appropriate shape factor depending on the environment of the fracture system.

Simulation and Modelling Consultancy Limited (SMC)

GENESYS is SMC's three-phase, 3D simulator designed to model both fractured and unfractured petroleum reservoirs.

In addition to the viscous and capillary forces, the matrix fracture exchange terms[5] handle gravity forces with different results depending on matrix block size or matrix block connections. The exchange terms and gravity forces within the exchange terms simulate the behavior of a single matrix block surrounded by fractures that might contain different fluids. Gravity forces were internally calculated as functions of saturation[5].

Several different choices of discretized time-solution techniques are available in GENESYS. Various sequential and IMPES solutions are obtained as simplified versions of the fully implicit technique. Ref. 16 provides the details of the conservation equations and the solution techniques.

Scientific Software-Intercomp (SSI)

SSI used SIMBEST II for this Project. This simulator was designed to expand traditional black-oil simulation to include dual-porosity and pseudo-compositional behavior.

In the dual-porosity option, the fluids transfer flow is presently modelled using a formulation described in Ref. 1.

SIMBEST II allows automatic accounting of phase pressure differences between the matrix and fracture when the matrix is subjected to capillary equilibrium and the fracture is in vertical equilibrium.

Well unknowns are normally treated fully implicitly at all times in SIMBEST II, but for expediency of implementation of the constant drawdown constraint specified for the present Project they were modelled explicitly at each non-linear iteration. As a result, more than twice as many non-linear iterations were required than would have been the case for other well operating constraints.

SIMBEST II employs both fully implicit and adaptive implicit non-linear formulations. For solving the sets of linear equations within each linear iteration either D-4 Gaussian elimination or a conjugate-gradient iterative solution package can be selected.

SIMBEST II does not have a pressure dependent gas-oil capillary pressure option. Gas-oil capillary pressures at 4000 psig [27.60 MPa] were used for the gas injection and depletion runs.

COMPARISON OF RESULTS

In line with the tradition of previous SPE Comparative Solution Projects[17–21], a minimum of commentary is presented on the results submitted by the ten participants of this Project.

Single Block Results

Figs. 1 and 2 show the results of single cell dual-porosity simulations by all ten participants of the Project, and the results of a fine grid single-porosity simulation. Fine grid simulations give a recovery of 40 percent for $P_{cf} = 0$, and 44 percent when $P_{cf} = 0.1$ psi (0.69 kPa) at the 5 year termination. Note that at the end of 5 years the results of the dual-porosity simulations for the majority of the participants are close to the single-porosity fine grid simulation.

Cross Sectional Results

Depletion. - Figs. 3 through 5 present oil production rate, produced GOR, and pressure as a function of time for the zero fracture capillary pressure run. Figs. 6 through 8 show the same plots for runs which used fracture capillary pressure based on the adjusted data of Table 4 (ECL and SSI used gas-oil capillary pressure data at 4000 psi [27.58 mPa]). With few exceptions, most models show similar trends in the reported results. A comparison of the zero and non-zero fracture capillary pressure results clearly indicates that capillary continuity has a major influence on both the produced GOR and reservoir pressure.

Reinjection. - Figs. 9 through 11 show oil production rate, produced GOR, and pressure as a function of time for the gas injection case when 90 percent of the produced gas is reinjected. These figures are based on the assumption of zero fracture capillary pressure. For the case of non-zero fracture capillary pressure the results are shown in Figs. 12, 13 and 14. Similar to the depletion runs, there is a noticeable variation between the results of the nine participants.

The reinjection runs, similar to the depletion runs, indicate a strong influence of fracture capillary pressure on the results. Table 5 presents the fracture and matrix gas saturations for all layers at I = 5 for the non-zero fracture capillary pressure run. Note that there is a substantial variation of fracture saturation in the top layers at time equal to 2 years.

Water Injection - Fig. 15 shows both the oil production rate and water cut as a function of time for the water injection test example. Unlike the previous runs, the results from all participants are in general agreement.

Time-Steps and Iterations

Table 6 lists the number of time steps and global iterations reported by the nine participants of the cross-sectional runs.

CONCLUDING REMARKS

Most of the current techniques in dual-porosity simulation have been used by the participants of this Comparative Solution Project. The results based on various techniques, we believe, will be of value in further enhancement of fractured reservoir simulation technology.

The comparison of solutions from various participants indicates that for some examples, there is a noticeable difference in the results. Different formulations for matrix fracture exchange is the main reason for this difference. The difference between the cases with zero and non-zero fracture capillary pressure indicates the need for further development of the physics and numerical modelling of naturally fractured petroleum reservoirs.

ACKNOWLEDGEMENTS

The authors wish to express their appreciation to the organizations participating in this Project. We would also like to thank T. N. Dixon and R. G. Pierson for their assistance in setting up the example problems and processing results for this Project.

NOMENCLATURE

- B - formation volume factor, RB/STB
- D_{ma} - depth of matrix
- D_f - depth of fracture
- I - grid block index in the x-direction
- J - grid block index in the y-direction
- K - grid block index in the z-direction
- k - permeability
- k_m - matrix permeability
- k_f - effective fracture permeability
- k_r - relative permeability
- L_{ma} - length of matrix block
- N_x - no. of grid blocks in the x-direction
- N_y - no. of grid blocks in the y-direction
- N_z - no. of grid blocks in the z-direction
- P_{cf} - fracture capillary pressure
- P_{cwo} - water-oil capillary pressure (matrix)
- r - radial distance from the center of a cylindrical grid block
- S_{ge} - matrix equilibrium gas saturation, fraction
- S_{gf} - fracture gas saturation, fraction
- S_{gm} - matrix gas saturation
- S_w - water saturation
- z - vertical distance for a cylindrical grid block
- Δp - drawdown, psi
- Δx - gridcell dimension in the x-direction
- Δy - gridcell dimension in the y-direction
- Δz - gridcell dimension in the z-direction
- μ - viscosity
- ϕ_f - fracture porosity
- ϕ_m - matrix porosity
- σ - shape factor

REFERENCES

1. Gilman, J. and Kazemi, H.: "Improvements in Simulation of Naturally Fractured Reservoirs", SPEJ (Aug. 1983) 675-707.
2. Kazemi, H., Merril, L.S., Porterfield, K.L., and Zeman, P.R.: "Numerical Simulation of Water-Oil Flow in Naturally Fractured Reservoirs", SPEJ (Dec. 1976) 317-326.
3. Thomas, L.K., Dixon, T.N. and Pierson, R.G.: "Fractured Reservoir Simulation", SPEJ (Feb. 1983) 42-54.
4. Litvak, B.L.: "Simulation and Characterization of Naturally Fractured Reservoirs", Prod. Reservoir Characterization Technical Conference, Dallas, Academic Press, New York City (1985).
5. Sonier, F., Bouillard, F., and Blaskovich, F.T.: "Numerical Simulation of Naturally Fractured Reservoirs", Paper SPE 15427 presented at the 1986 SPE Annual Technical Conference and Exhibition, New Orleans, Oct. 5-8.
6. Dean, R.H., and Lo, L.L.: "Simulation of Naturally Fracture Reservoirs", SPERE (May 1988) 638-648.
7 Rossen, R.H., and Shen, E.I.: "Simulation of Gas/Oil Drainage and Water/Oil Imbibition in Naturally Fractured Reservoirs", Paper SPE 16982 presented at the 1987 SPE Annual Technical Conference and Exhibition, Dallas, TX, Sept. 27-30.
8. Saidi, A.M.: "Simulation of Naturally Fractured Reservoirs", Paper SPE 12270 presented at the 1983 SPE Symposium on Reservoir Simulation, San Francisco, Nov. 16-18.
9. Pruess, K. and Narashimhan, T.N.: "A Fractical Method for Modelling Fluid and Heat Flow in Fractured Porous Media", SPEJ (Feb. 1985) 14-26.
10. Horie, T., Firoozabadi, A., and Ishimotot, K.: "Capillary Continuity in Fractured Reservoirs", Paper SPE 18282 presented at the 1986 SPE Annual Technical Conference and Exhibition, Houston, Oct. 2-5.

11. Chen, W.H., Wasserman, M.L., and Fitzmarris, R.E.: "A Thermal Simulator for Naturally Fractured Reservoirs", Paper SPE 16008 presented at the 1987 SPE Symposium on Reservoir Simulation, San Antonio, TX, Feb. 1-4.
12. Gilman, J.R.: "An Efficient Finite Difference Method for Simulating Phase Segregation in Matrix-Blocks in Double Porosity Reservoirs", SPERE (July 1986) 403-413.
13. Beckner, B.L., Firoozabadi, A., and Aziz, K.: "Modelling Transverse Imbibition in Double-Porosity Simulators", Paper SPE 17414 presented at the 1988 SPE California Regional Meeting, Long Beach, CA, March 23-25.
14. Quandalle, P., and Sabathier, J.C.: "Typical Features of a New Multipurpose Reservoir Simulator", Paper SPE 16007 presented at the 1987 SPE Symposium on Reservoir Simulation, San Antonio, TX, Feb. 1-4.
15. Warren, J.E., and Root, P.J.: "The Behavior of Naturally Fractured Reservoirs", SPEJ, (Sept. 1963) 245-255.
16. Sonier, F., and Eymard, R.: "A New Simulator for Naturally Fractured Reservoirs", Paper SPE 16006, presented at the 1987 SPE Symposium on Reservoir Simulation, San Antonio, TX, Feb. 1-4.
17. Odeh, A.S.: "Comparison of Solutions to a Three-Dimensional Black-Oil Reservoir Simulation Problem", JPT (Jan. 1981) 13-25.
18. Weinstein, H.G., Chappeleart, J.E., and Nolen J.S.: "Second Comparative Project: A Three-Phase Coning Study", JPT (March 1986) 345-353.
19. Kenyon, D.E., and Behie, G.A.: "Third SPE Comparative Solution Project: Gas Cycling of Retrograde Condensate Reservoirs", JPT (Aug. 1987) 981-998.
20. Aziz, K., Ramesh, B., and Woo, P.T.: "Fourth SPE Comparative Solution Project: A Comparison of Steam Injection Simulators", JPT (Dec. 1987) 1576-1584.
21. Killough, J. and Kossak, C.: "Fifth SPE Comparative Solution Project: Evaluation of Miscible Flood Simulators". Paper SPE 16000, presented at the 1987 SPE Symposium on Reservoir Simulation, San Antonio, TX, Feb. 1-4.

APPENDIX

Participants in the Sixth SPE Comparative Solution Project:

1. Chevron Oil Field Research Company (Chevron)
   P. O. Box 446
   La Habra, CA 90633, U.S.A.

2. Computer Modelling Group (CMG)
   3512 - 33 Street, N.W.
   Calgary, Alberta
   Canada, T2L 2A6

3. DANCOMP A/S
   Bregnerodvej 132
   DK-3460 Birkerod, Denmark

4. Exploration Consultants Limited (ECL)
   Highlands Farm
   Henley-on-Thames, England

5. FRANLAB
   Rue Albert Einstein
   Sophia Antipolis
   P. O. Box 14
   06561 Valbonne Cedex, France

6. Japan Oil Engineering Company (JOE)
   Riccar Building, 2 - 1
   Ginza, 6-Chome, Chuo-ku
   Tokyo, Japan

7. Marathon Oil Company
   P. O. Box 269
   Littleton, Colorado 80160-0269 U.S.A.

8. Phillips Petroleum Company
   141 Geoscience Building
   Bartlesville, OK 74004, U.S.A.

9. Scientific Software-Intercomp (SSI)
   1801 California Street
   3rd Floor
   Denver, CO 80202-2699 U.S.A.

10. Simulation and Modelling Consultancy Limited (SMC)
    Crown House, 9th Floor, London Road,
    Morden Surrey SM4 5DX
    England

TABLE 1 - Matrix Water-Oil Capillary Pressure Data

S_w	P_{cwo}, psi [kPa]
0.20	1.0 [6.89]
0.25	0.5 [3.45]
0.30	0.3 [2.07]
0.35	0.15 [1.03]
0.40	0.00 [0.00]
0.45	-0.2 [-1.38]
0.50	-1.2 [-8.27]
0.60	-4.0 [-27.0]
0.70	-10.0 [-6.89]
0.75	-40.0 [-275.0]

TABLE 3 - Basic Date

$k_m = 1$ md, $\phi_m = 0.29$, $\phi_f = 0.01$

Layer Data

Layer	Effective Fracture Permeability k_f, md	Block Height ft [m]	PI*, $\frac{RB \cdot cp}{D \cdot psi}$
1	10	25 [7.62]	1
2	10	25 [7.62]	1
3	90	5 [1.52]	9
4	20	10 [3.05]	2
5	20	10 [3.05]	2

$N_x = 10$ $N_y = 1$ $N_z = 5$

$\Delta x = 200$ ft [61 m], $\Delta y = 1000$ ft [305 m], $\Delta z = 50$ ft [15.2 m]

z-direction transmissibilities, multiply calculated values times 0.1.

Initial reservoir pressure (1, 1, 1) = 6000 psig [41.37 MPa]

* Rate = $\frac{k_r PI}{B\mu}$: Δp, in psi, μ in cp, B in RB/STB, and Rate in STB/D.

TABLE 2 - Matrix Block Shape Factors*

Block Size, ft [m]	Water-Oil Shape Factor, ft^{-2} [m^{-2}]
5 [1.52]	1.000 [10.76]
10 [3.05]	0.250 [2.69]
25 [7.62]	0.040 [0.43]

* The basis for the selection of the above shape factors is given in Ref. 3. Participants were given the choice to use a single shape factor for a given block size for both water-oil and gas-oil cases or different values for the two cases. Some techniques do not use the shape factors at all.

TABLE 4 - Fracture Capillary Pressure Data

S_g	P^*_{cfgo}, psi [kPa]
0.0	0.0375 [0.258]
0.10	0.0425 [0.293]
0.20	0.0475 [0.327]
0.30	0.0575 [0.396]
0.40	0.0725 [0.500]
0.50	0.0880 [0.607]
0.70	0.1260 [0.869]
1.0	0.1930 [1.331]

Fracture water-oil capillary pressure is equal to zero. Fracture relative permeability curves are straight lines with zero residuals.

* at the bubblepoint pressure of 5,545 psig [38.23 MPa].

TABLE 5 - Cross Sectional Gas Reinjection Non-Zero P_{cf} Results*

TIME YEARS	LAYER	PHILLIPS		CMG		SMC		MARATHON		FRANLAB		ECL		CHEVRON		SSI		DANCOMP	
		S_{gf}	S_{gm}	S_{gf}	S_{gm}	S_{gf}	S_{gm}	S_{gf}	S_{gm}	S_{gf}	S_{gm}	S_{gf}	S_{gm}	S_{gf}	S_{gm}	S_{gf}	S_{gm}	S_{gf}	S_{gm}
2	1	0.194	0.094	0.384	0.111	0.245	0.111	0.617	0.102	0.249	0.090	0.344	0.135	0.065	0.093	0.697	0.076	0.333	0.093
	2	0.174	0.083	0.212	0.061	0.210	0.094	0.519	0.080	0.145	0.068	0.308	0.115	0.078	0.097	0.649	0.062	0.198	0.069
	3	0.146	0.048	0.100	0.034	0.175	0.044	0.144	0.063	0.087	0.065	0.267	0.022	0.135	0.058	0.344	0.029	0.109	0.042
	4	0.022	0.014	0.019	0.041	0.026	0.025	0.004	0.060	0.010	0.030	0.027	0.016	0.008	0.047	0.009	0.035	0.009	0.031
	5	0.017	0.012	0.017	0.039	0.020	0.024	0.003	0.059	0.008	0.028	0.019	0.016	0.007	0.045	0.007	0.034	0.007	0.030
5	1	0.566	0.284	0.650	0.273	0.573	0.290	0.679	0.249	0.665	0.251	0.618	0.301	0.679	0.268	0.789	0.191	0.590	0.270
	2	0.514	0.255	0.595	0.229	0.520	0.261	0.625	0.221	0.610	0.225	0.560	0.270	0.652	0.263	0.754	0.172	0.536	0.231
	3	0.407	0.151	0.454	0.137	0.418	0.168	0.470	0.165	0.453	0.169	0.393	0.120	0.493	0.156	0.505	0.113	0.393	0.142
	4	0.021	0.009	0.049	0.037	0.025	0.012	0.023	0.095	0.025	0.039	0.019	0.012	0.067	0.037	0.019	0.059	0.020	0.027
	5	0.014	0.007	0.038	0.037	0.015	0.011	0.014	0.095	0.015	0.034	0.012	0.011	0.023	0.035	0.011	0.058	0.013	0.026
10	1	0.820	0.436	0.805	0.413	0.873	0.433	0.809	0.396	0.853	0.387	0.873	0.431	0.855	0.400	0.889	0.301	0.843	0.428
	2	0.791	0.413	0.788	0.382	0.830	0.418	0.780	0.371	0.827	0.370	0.834	0.414	0.835	0.390	0.871	0.286	0.773	0.409
	3	0.718	0.334	0.721	0.366	0.824	0.412	0.825	0.360	0.851	0.410	0.764	0.390	0.868	0.416	0.867	0.400	0.681	0.365
	4	0.025	0.004	0.068	0.023	0.122	0.005	0.242	0.089	0.200	0.032	0.047	0.009	0.285	0.019	0.282	0.064	0.032	0.021
	5	0.008	0.002	0.027	0.023	0.007	0.003	0.012	0.055	0.010	0.011	0.008	0.008	0.009	0.015	0.010	0.056	0.013	0.014
20	1	1.000	0.513	0.994	0.508	1.000	0.483	0.992	0.482	0.990	0.468	0.997	0.495	0.995	0.466	0.970	0.400	0.966	0.522
	2	1.000	0.508	0.990	0.501	1.000	0.480	0.982	0.475	0.988	0.464	0.994	0.493	0.994	0.464	0.964	0.393	0.962	0.519
	3	1.000	0.464	0.998	0.463	1.000	0.468	0.997	0.439	0.998	0.453	0.999	0.466	0.999	0.447	0.986	0.448	0.956	0.530
	4	0.527	0.173	0.528	0.170	0.605	0.284	0.770	0.309	0.656	0.309	0.513	0.242	0.619	0.276	0.760	0.290	0.410	0.140
	5	0.007	0.001	0.040	0.013	0.059	0.001	0.060	0.032	0.093	0.003	0.011	0.007	0.008	0.076	0.062	0.047	0.023	0.008

* Saturations at (5,1,1-5)

TABLE 6 - Total Number of Time Steps and Global Iterations

COMPANY	DEPLETION ZERO P_{cfgo}		DEPLETION NON-ZERO P_{cfgo}		REINJECTION ZERO P_{cfgo}		REINJECTION NON-ZERO P_{cfgo}		WATER INJECTION	
	STEPS	ITERATIONS	STEPS	ITERATIONS	STEPS	ITERATIONS	STEPS	ITERATIONS	STEPS	ITERATIONS
PHILLIPS	48	116	103	215	42	114	86	209	92	185
CMG	63	239	103	392	48	317	94	535	100	215
SMC	53	265	91	455	149	745	280	1400	170	550
MARATHON	66	140	106	290	34	119	91	444	96	260
FRANLAB	60	200	114	344	85	129	199	306	100	240
ECL	103	384	103	304	101	563	89	560	134	383
CHEVRON	36	196	104	495	22	228	89	576	88	540
SSI	75	308	106	424	106	424	96	384	100	400
DANCOMP	50	260	111	359	273	1201	576	2499	750	1505

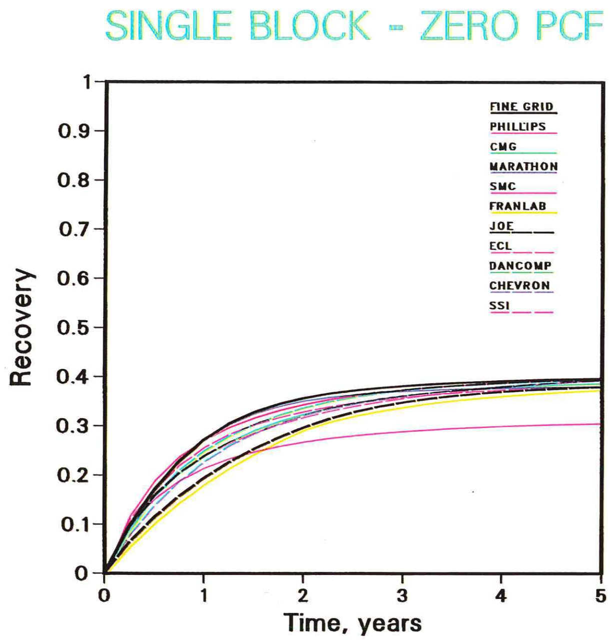

Fig. 1—Recovery vs. time, single block—Zero P_{cf}.

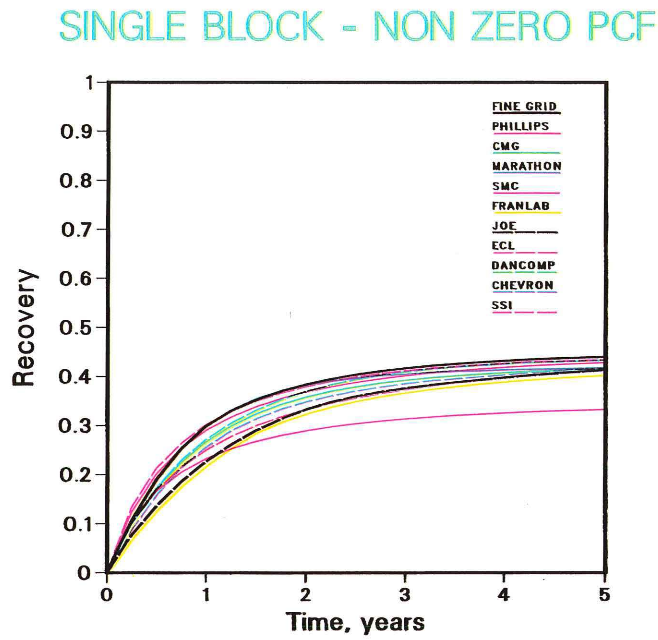

Fig. 2—Recovery vs. time, single block—Non-Zero P_{cf}.

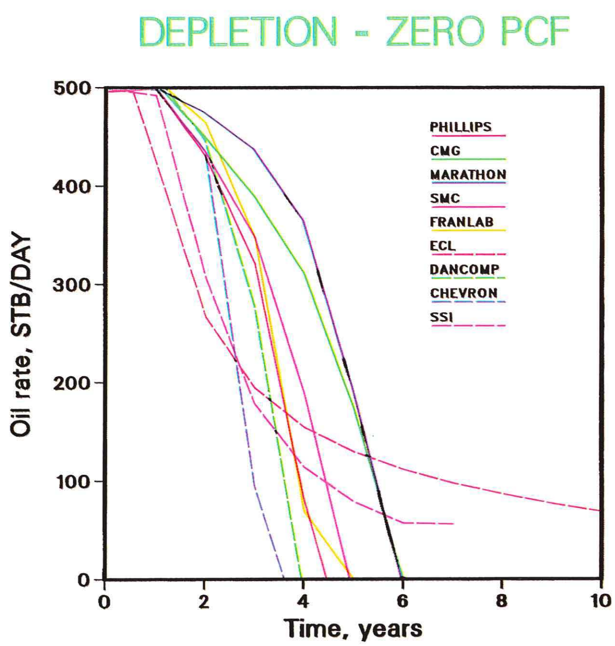

Fig. 3—Oil rate vs. time, depletion—Zero P_{cf}.

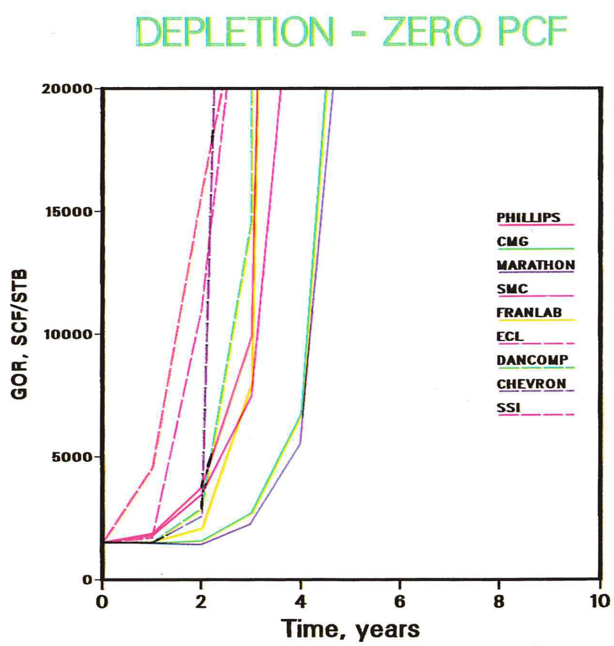

Fig. 4—Gas/oil ratio vs. time, depletion—Zero P_{cf}.

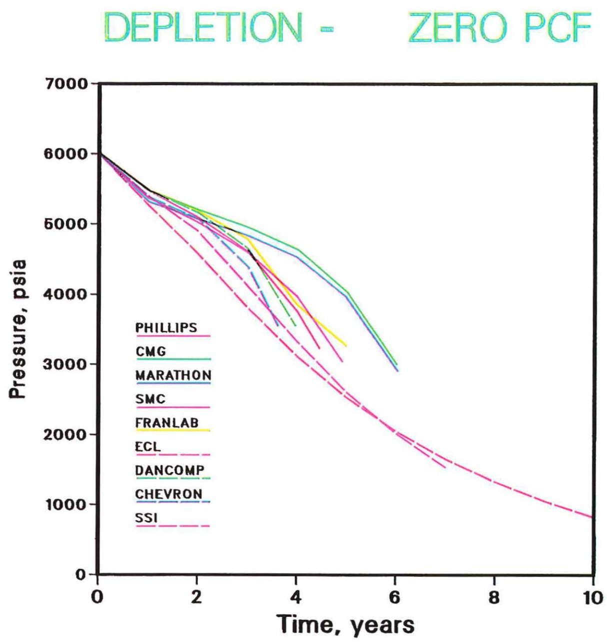

Fig. 5—Pressure vs. time, depletion—Zero P_{cf}.

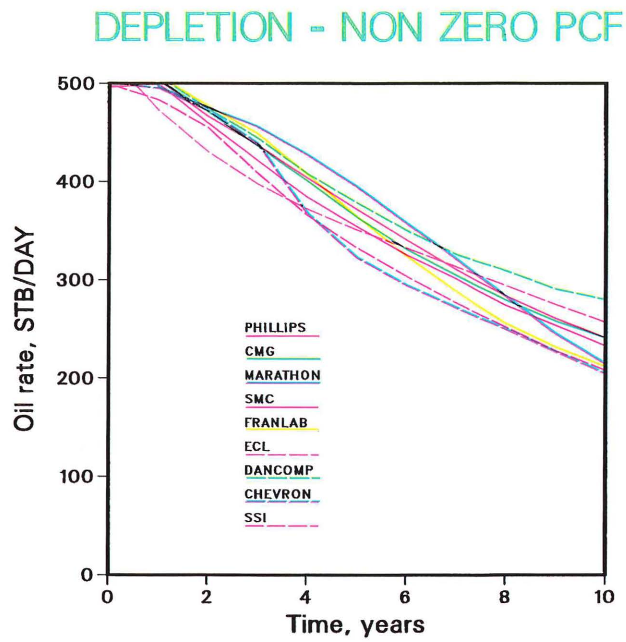

Fig. 6—Oil rate vs. time, depletion—Non-Zero P_{cf}.

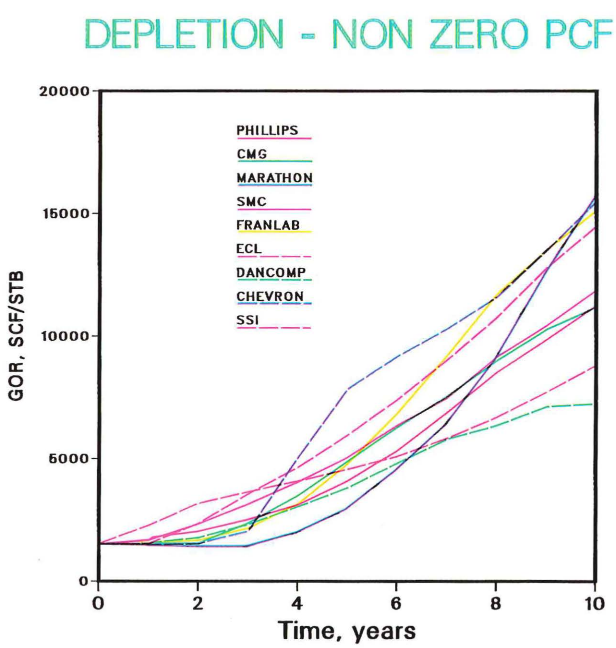

Fig. 7—Gas/oil ratio vs. time, depletion—Non-Zero P_{cf}.

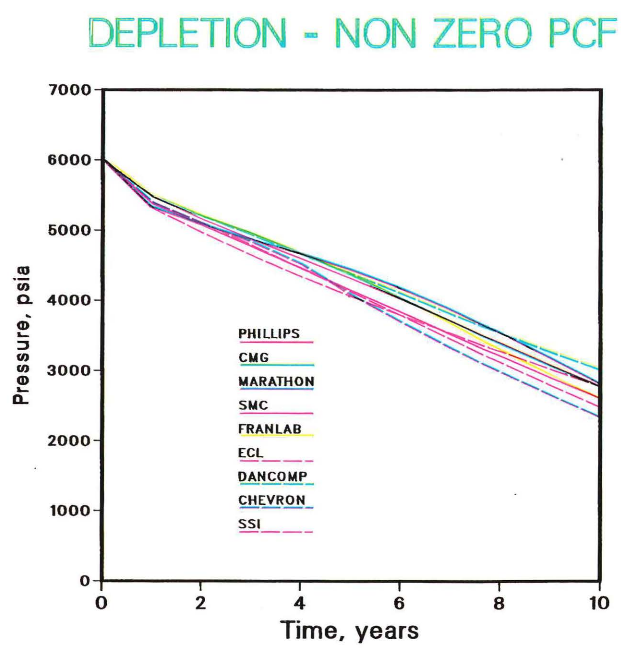

Fig. 8—Pressure vs. time, depletion—Non-Zero P_{cf}.

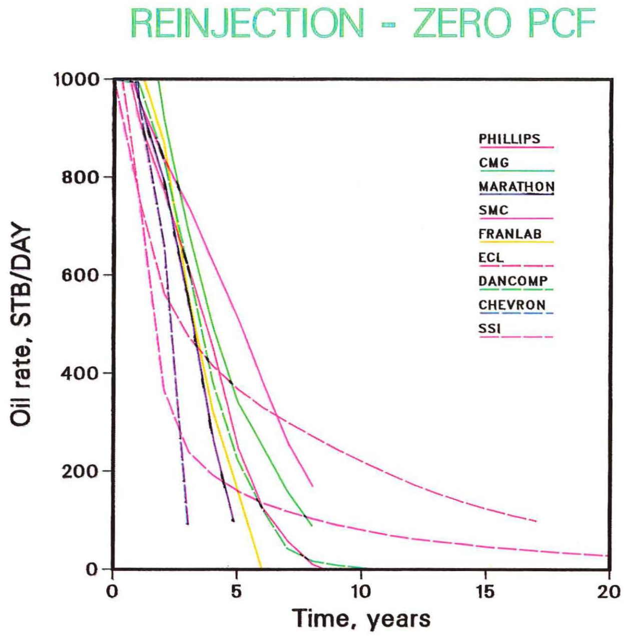

Fig. 9—Oil rate vs. time, gas reinjection—Zero P_{cf}.

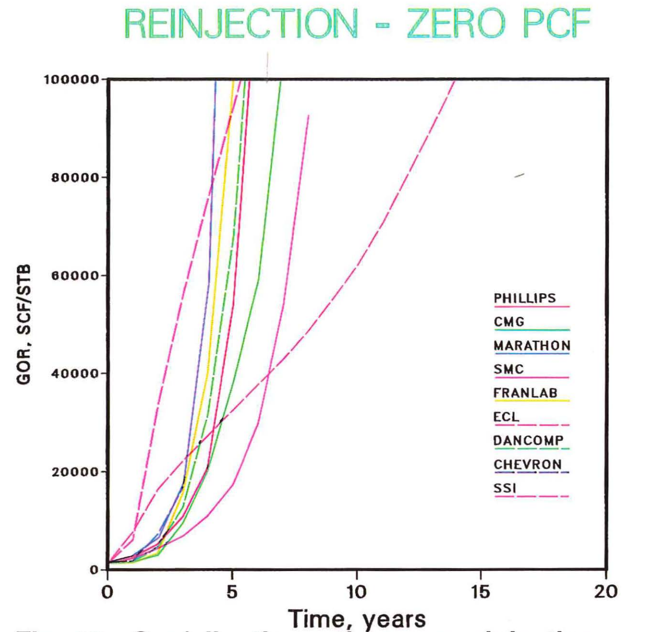

Fig. 10—Gas/oil ratio vs. time, gas reinjection—Zero P_{cf}.

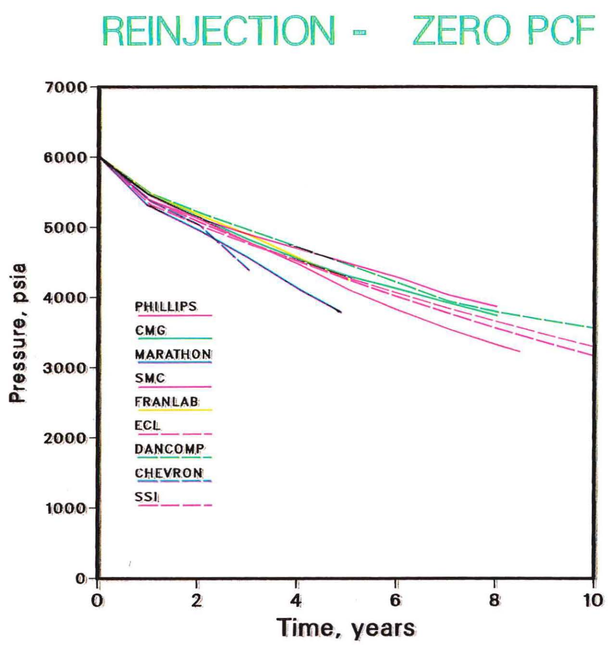

Fig. 11—Pressure vs. time, gas reinjection—Zero P_{cf}.

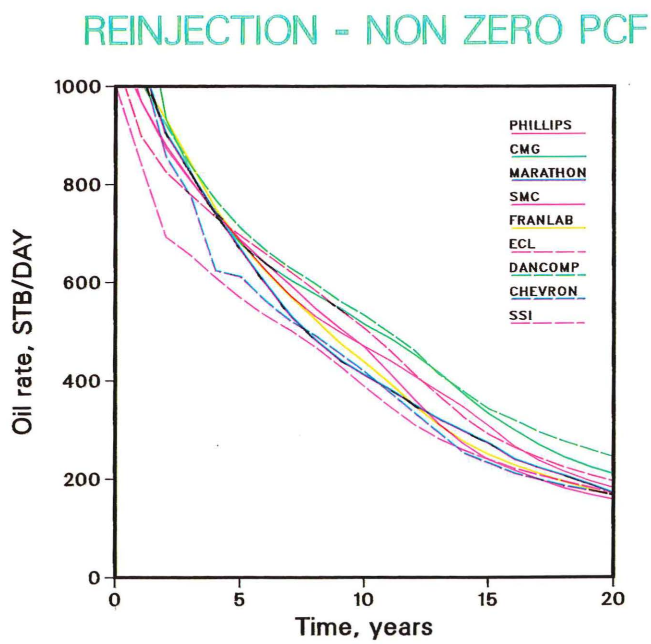

Fig. 12—Oil rate vs. time, gas reinjection—Non-Zero P_{cf}.

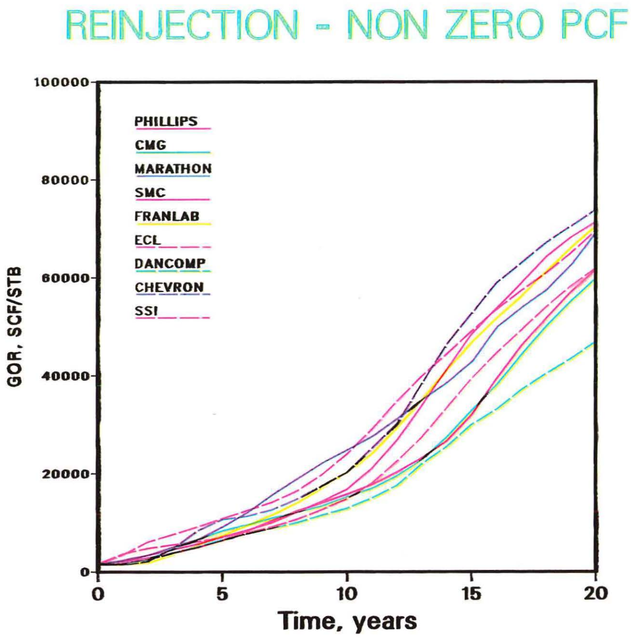

Fig. 13—Gas/oil ratio vs. time, gas reinjection—Non-Zero P_{cf}.

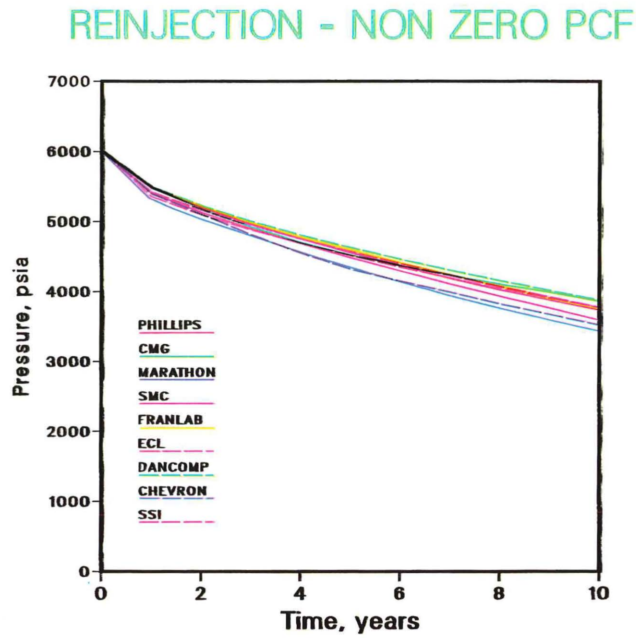

Fig. 14—Pressure vs. time, gas reinjection—Non-Zero P_{cf}.

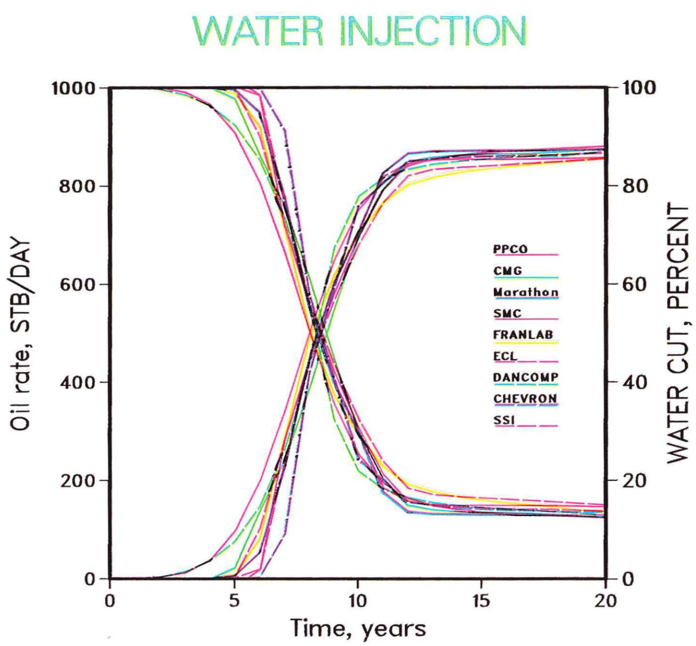

Fig. 15—Oil rate and water cut vs. time, water injection.